

Fluorimetric and Quasi-Elastic Light Scattering Study of the Solubilization of Nonpolar Low-Molar Mass Compounds into Water-Soluble Block-Copolymer Micelles

D. Kiserow,[†] K. Prochazka,[‡] C. Ramireddy,[†] Z. Tuzar,[§] P. Munk,[†] and S. E. Webber^{*†}

Department of Chemistry and Biochemistry and Center for Polymer Research, University of Texas at Austin, Austin, Texas 78712, Department of Physical Chemistry, Faculty of Science, Charles University, Albertov 2030, 12843 Prague 2, Czechoslovakia, and Institute of Macromolecular Chemistry, Czechoslovak Academy of Sciences, 16206 Prague 6, Czechoslovakia

Received June 6, 1991; Revised Manuscript Received August 7, 1991

ABSTRACT: The diblock copolymer polystyrene-*block*-poly(*tert*-butyl methacrylate) was prepared by anionic polymerization, and a portion was hydrolyzed to prepare polystyrene-*block*-poly(methacrylic acid). Some of the copolymers were end-tagged with either less than one on average or a chain of four 2-vinylnaphthalene moieties at the end of the polystyrene block, while others were tagged with exactly one dansyl group via the SO₂ linkage at the end of the poly(methacrylic acid) block. Micelles were initially prepared in mixtures of H₂O/1,4-dioxane (80 vol %) and then dialyzed into water to remove the dioxane. Steady-state and time-dependent fluorescence spectroscopy along with static and quasi-elastic light scattering (QELS) were used to study the solubilization of organic molecules into the micelles for different pHs, ionic strengths, and copolymer concentrations. It was found that a weight ratio of up to 5:1 solubilized benzene to polystyrene can be taken up by these micelles. Light scattering and fluorimetric measurements indicate that solubilization occurs simultaneously into micellar cores and into hydrophobic domains in the shells. Moreover, it is likely that the swelling of the micellar core and the increase in the core volume are partially compensated for by the decrease in shell thickness possibly due to an increased amount of hypercoiled-hydrophobic structure. Probe mobility was monitored by following excimer formation and the time-dependent fluorescence anisotropy of naphthalene in the cores and dansyl in the shells. The fluorescence properties proved to be sensitive indicators of core swelling during solubilization. It was also found that dansyl labels experience a much more complex and less polar microenvironment than expected for an aqueous medium. QELS and viscosity measurements indicate that, at low ionic strength and at a relatively low degree of neutralization of the carboxylic acid groups, the electrostatic repulsion of highly charged spherical micelles results in the formation of long-range order in micellar solutions.

Introduction

The associational and conformational properties of water-soluble polymers and copolymers are of great interest with respect to both self-assembly and solubilization phenomena. If well understood, these properties could be exploited in the controlled uptake and release of drugs, pollutants, and other compounds which may be important from biological and/or environmental points of view. Steady-state and time-resolved fluorescence measurements have proven to be useful techniques for the investigation of sorption/desorption processes as well as other phenomena, and there are many applications of these methods within this field.¹ Fluorescence from polarity-sensitive probes (or more generally environment-sensitive probes) such as dansyl and pyrene can be studied, resulting in a greater understanding of the microenvironment of a probe, i.e., the structural properties of the "binding site".²

There have been various studies on polysoaps (alternating polyelectrolytes with nonpolar comonomers).³ However, investigations of water-soluble block-copolymer micelles are much less abundant^{1d} despite the fact that they represent excellent systems for the solubilization of organic substances. One reason for the scarcity of data is the difficulty of preparation of well-defined amphiphilic block copolymers with a uniform molar mass distribution within the blocks. These conditions on copolymer struc-

ture are necessary in order to be able to perform reproducible physicochemical measurements and monitor the controlled uptake and release of molecules with the system.

Solubilization of various polymeric substances into nonpolar block copolymer micelles in organic solvents has been studied in detail.⁴ It has been shown that if a homopolymer is identical in chemical structure to the insoluble core block and has a molar mass lower or equal to that of the insoluble block, it may be solubilized into micellar cores. While small molecules may also be solubilized into these micelles, practical applications are limited because of the extensive solubility of those compounds in the organic solvent phase. This is not the case for water-soluble micelles, however. Almost all solubilization studies on water-soluble block-copolymer micelles have focused on poly(propylene oxide)-*block*-poly(ethylene oxide) or on other copolymers with water-soluble poly(ethylene oxide) blocks.⁵ Nagarajan et al. have shown that block copolymer micelles have a much higher capacity for solubilizing certain organic substances than detergent micelles.^{5b} They are also highly selective, which may be explained by the thermodynamics of polymer mixtures when taking into account the interaction parameter (χ). Studies describing the solubilization of water into poly(ethylene oxide) cores of polystyrene-*block*-poly(ethylene oxide) micelles in cyclohexane have been carried out by Cogan et al.⁶

In this paper we report the solubilization of organic substances into a water-soluble copolymer with polystyrene and poly(methacrylic acid) blocks. Several copolymer

* To whom correspondence should be addressed.

[†] University of Texas at Austin.

[‡] Charles University.

[§] Czechoslovak Academy of Sciences.

Table I
Molecular Characteristics of Diblock Copolymers

copolymer	$10^{-3}M_w$ (g mol ⁻¹)	M_w/M_n^a	x_S^b	x_H^b
N4-SMA	60.3	1.08	0.45	0.98
N1-SMA	67.2	1.11	0.59	0.97
D1-SMA	44.9	1.10	0.54	1.00
SMA	57.8	1.06	0.60	1.00

^a M_w and M_n measured by SEC. ^b Molar fraction of polystyrene (x_S) and degree of hydrolysis (x_H) measured by NMR.

samples differing in fluorescence labeling have been used in this study for comparison.

When compared with copolymer micelles containing water-soluble poly(ethylene oxide) shells, the behavior of the systems studied here is considerably more complicated. Micellar behavior is modified not only by the highly non-polar polystyrene core but also by the polyelectrolyte nature⁷ and significant "specific interactions" in the poly-(methacrylic acid) shell.⁸ These interactions are similar to those observed for alternating copolymers of maleic acid and alkyl vinyl ethers with bulky alkyl groups.⁹ The behavior of dilute solutions of poly(methacrylic acid) under various conditions (differing pH, ionic strength, etc.) has been studied in detail by many authors for nearly half a century,⁸ leading to a broad understanding of its properties. However, controversy persists in the interpretation of the nature of hypercoiling at low pH as to whether or not the hypercoiling is a progressive or a cooperative process. The properties of semidilute solutions of poly(methacrylic acid) have been studied in detail by only a few authors.⁷ The micelles investigated here have concentrated poly-(methacrylic acid) shells because of the fact that all the ends of the poly(methacrylic acid) blocks are fixed in a narrow layer close to the core/shell interface and the chains are partially radially oriented. As far as we know, similar systems have not yet been studied.

Experimental Section

Polymers. The diblock polystyrene-*block*-poly(methacrylic acid) copolymers (SMA) were prepared by the anionic polymerization of styrene and *tert*-butyl methacrylate in tetrahydrofuran at -78 °C using cumylpotassium as an initiator with subsequent hydrolysis in a mixture of HCl/1,4-dioxane and tagged with 2-vinylnaphthalene as described previously.¹⁰ The naphthalene-tagged diblock copolymers, N1-SMA and N4-SMA, contain on average either less than one 2-vinylnaphthalene unit per chain or a short chain of four 2-vinylnaphthalene units, respectively. In both cases, the labels are attached to the end of the polystyrene block. Because of the statistical nature of the polymerization reaction, the number of labels per chain represents the average value of a Poisson distribution.¹⁰ The dansyl-tagged sample, D1-SMA, contains precisely one dansyl per copolymer chain attached via the SO₂ group at the end of the poly-(methacrylic acid) block. The bonding of dansyl occurs by terminating the living polymerization of the *tert*-butyl methacrylate block with dansyl chloride (purchased from Aldrich) instead of methanol. Hydrolysis of the poly(*tert*-butyl methacrylate) by HCl results in a considerable fraction of protonated (CH₃)₂N groups on the dansyl moieties. As will be discussed later, this greatly complicated the photophysics of this species. Characterization of the copolymer samples by SEC and NMR was performed as described previously¹⁰ (see Table I for details).

Block Copolymer Micelles. All micelles were prepared by direct dissolution of the samples in a mixture of H₂O/1,4-dioxane (80 vol %) with stepwise dialysis into mixtures richer in water (always by 10 vol %). Dialysis was repeated until the samples were present in pure water or aqueous buffers (see Table II for details).

Solvents. Spectral grade 1,4-dioxane, analytical grade benzene, toluene, and analytical grade buffer solutions were used as purchased (Aldrich). Deionized water was used to prepare aqueous solvents.

Table II
Characteristics of Block-Copolymer Micelles in a Dilute Aqueous Solution^a

copolymer	$10^{-6}(M_w^{app})_M^b$ (g mol ⁻¹)	R_H^c (nm)
N4-SMA	3.2	16.8
N1-SMA	15	44
D1-SMA	13	18.9
SMA	15	46

^a $c = 3 \times 10^{-3}$ g cm⁻³. ^b Apparent molar mass of micelles ($(M_w^{app})_M$) measured by static light scattering. ^c Apparent hydrodynamic radius of micelles (R_H) measured by QELS.

Fluorescence Spectroscopy. Steady-state fluorescence spectra were recorded on a SPEX Fluorolog fluorimeter system described elsewhere.¹⁰

Lifetime measurements and fluorescence-depolarization measurements were performed by the method of time-correlated single-photon counting as described elsewhere.¹⁰ The MCB has 8192 channels and the time resolution is ca. 6.7 ps/channel for anisotropy measurements and ca. 27 ps/channel for lifetime measurements. Lifetime measurements were made with the polarizer at the magic angle (54.7°) to ensure the proper ratio of parallel to perpendicular intensity was observed. For depolarization measurements, the polarizer was rotated from horizontal to vertical every 5 min live time¹¹ while collecting data, and this process continued until the desired number of counts was reached. This procedure minimized any perturbations that would occur in data collected for long times (typically 2 h or more) due to system instability. Other details on the apparatus, data acquisition, mathematical treatment, etc., are described elsewhere.¹⁰

The typical apparent OD for labeled micelle solutions were ca. 1.0 for fluorescence measurements (partially due to significant light scattering). Degassing of selected micellar solutions did not result in significant changes in intensities and lifetimes; thus, for the measurements reported here the solutions were not degassed.

Static and Quasi-Elastic Light Scattering (QELS). The weight-average molar masses of copolymer and micelles were measured by a Sofica 42000 apparatus as described elsewhere.¹² The apparent hydrodynamic radii (R_H) of both micelles and unimers (measured at a low, albeit finite concentration) were measured with a Brookhaven BI 2030 apparatus with a 72-channel correlator and a He-Ne laser as a light source. The R_H values were obtained using the cumulant method of the data treatment based on

$$g^{(1)}(q, t) = \exp[-\Gamma(q)t + 0.5\mu_2(q)t^2 + \dots] \quad (1)$$

where q is the scattering vector and t is the sampling time. From the first term, the diffusion coefficient (D) may be obtained using a relation

$$D = \Gamma(q)/q^2 \quad (2)$$

and the apparent hydrodynamic radius (R_H) may be calculated from the Stokes-Einstein relation

$$R_H = kT/(6\pi\eta D) \quad (3)$$

where k is Boltzmann's constant, T the temperature, and η the solvent viscosity. The second moment of the correlation curve ($\mu_2(q)$) is proportional to the polydispersity index (P_D) of the diffusion coefficient distribution where

$$P_D = \mu_2(q)/[\Gamma(q)]^2 \quad (4)$$

Since the computed values represent the z average of the reciprocal value of the hydrodynamic radius ($(R_H^{-1})_z$) and micellization in pure water and buffers is significantly shifted in favor of micelles, the values measured in water-rich media correspond to those of micelles.¹⁰

For micellar solutions with partially neutralized carboxylic groups at low ionic strength, the interpretation of QELS measurements cannot be based exclusively on the theory of simple diffusion of individual, weakly interacting spherical particles. All experimental techniques used here indicate a high degree of organization of the system. The apparent values of R_H obtained

using the assumption of simple diffusion are quite high, and the experimental data indicate a very high polydispersity in diffusion coefficients. The correlation curves ($g^{(1)}(t, q)$), are strongly non-exponential and decay significantly faster at short times than at long times. The two distinct characteristic times differ so greatly in their time scales that two diffusion coefficients have been unambiguously distinguished. This is despite limited resolution due to the small number of correlation channels for data acquisition (72), together with only moderately sophisticated software for data treatment.

Ultracentrifugation. The sedimentation velocity measurements were performed using a Spinco Model E analytical ultracentrifuge with Schlieren optics as described elsewhere.¹⁰

Results and Discussion

Solubilization into Micellar Cores. A Study with QELS. At this time, a broad and general set of experimental data describing the solubilization of organic compounds into water-soluble block-copolymer micelles does not exist. A comparison with studies done on different systems, mainly with the relatively general study by Nagarajan et al.^{5a,b} on polystyrene-*block*-poly(ethylene oxide), indicates that the solubilization processes in micelles with poly(methacrylic acid) shells differ considerably from those of other types of copolymer micelles.

Nagarajan et al. solubilized aromatic hydrocarbons and other organic substances into polystyrene cores by shaking relatively concentrated aqueous micellar solutions with an organic liquid that was immiscible with water. By analyzing both equilibrium phases by gas chromatography after a sufficiently long equilibration time (1 h), they found the mass ratio of solubilized organic substance to polystyrene (denoted ξ_B in this study) was approximately 1 for toluene and 2 for benzene.

Our attempts to reproduce the aforementioned procedure with benzene, toluene, and our block copolymers in pure water and neutral and slightly acidic buffers failed. Similarly, all experiments investigating the possibility of solubilizing benzene rapidly into micelles (both continuously and by the stepwise addition of microvolumes of benzene into micellar solutions) were unsuccessful. The addition of volumes that were smaller than those corresponding to previously published data⁵ resulted in the precipitation of a significant fraction of copolymer. We observed that one must initially add only a very small volume of an aromatic hydrocarbon, corresponding roughly to its solubility in water, and the solution must be equilibrated (by stirring or shaking) for at least 1 h. Then, very small portions may be added slowly at about 1-h intervals. If precipitation is to be avoided, less than 3 μ L of benzene should be added to 3 mL of a micellar solution in a single step (for a copolymer concentration of $(3-5) \times 10^{-3}$ g cm⁻³). When this procedure is carefully followed, relatively high loadings of benzene in micelles may be reached depending on the copolymer concentration, pH, ionic strength, etc. (see below). The highest loadings we achieved greatly exceeded the limiting amounts of solubilized benzene for micelles with poly(ethylene oxide) shells as reported by Nagarajan et al.^{5a,b} An interesting observation was that micellar systems were most sensitive to precipitation during the early stages of benzene addition; this was confirmed under different experimental conditions. Under conditions which allow one to safely overstep the "critical precipitation region" (see below), large volumes of aromatic hydrocarbons may be added rapidly (close to the saturation limit) and no precipitation is observed above the saturation limit. Two phases form as the amount of hydrocarbon added to the solution increases. One is an aqueous phase containing swollen micelles, and the other

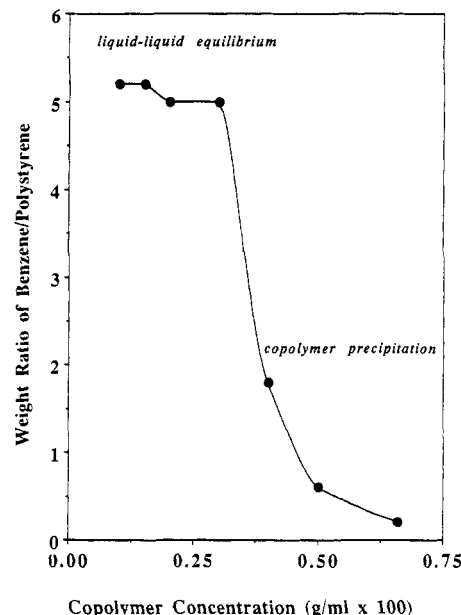


Figure 1. Solubilization limits of benzene into micelles in pure water expressed as the weight ratio of benzene to polystyrene (ξ_B) as a function of copolymer concentration (g/mL).

is an organic phase. The latter may contain a small fraction of copolymer and has the potential to form a microemulsion.

At high pH, part of the poly(methacrylic acid) blocks are charged and presumably stretched out. The micellar systems are quite stable, and direct shaking with a surplus of organic liquid is possible, resulting in the solubilization of considerable amounts of organic substances into micellar cores without any precipitation. Evidently, the state of ionization of the poly(methacrylic acid) shell has a large effect on the micelle stability.

The solubilization and stability limits of these systems were studied for various pH and copolymer concentrations. It is difficult to determine the saturation limit and the appearance of a very small volume of a second phase. The results of all the experimental techniques (particularly QELS and ultracentrifugation) show that no microemulsion is formed at high benzene loadings before phase separation occurs. The hydrodynamic diameter ($2R_H$), polydispersity (μ_2/Γ^2), and apparent sedimentation coefficient (s) change slowly and smoothly with an increasing benzene loading. They slowly approach limiting values at high ξ_B (benzene to polystyrene weight ratio) and this fact hinders the precise estimation of the solubilization limits. Figure 1 shows the "solubilization phase diagram" of H₂O/D1-SMA/benzene at 25 °C. At higher concentrations, micelles swollen by benzene are not stable and macroscopic precipitation of copolymer occurs at relatively low benzene loadings. For lower copolymer concentrations, much higher benzene loadings may be reached and two liquid phases are formed without any observable precipitation: (1) an aqueous solution of swollen micelles and (2) an organic phase (benzene). Saturation data presented here are corrected for the solubility of benzene in water (0.07 wt %). It should be noted, however, that until the saturation of micelles by benzene is reached, the concentration of benzene in water is probably lower than 0.07 wt %. This is due to having a complex phase equilibrium for a multicomponent system with copolymer micelles which have a high affinity for benzene, instead of having a binary benzene/water equilibrium.

General data describing the solubilization of aromatic hydrocarbons into polystyrene-*block*-poly(methacrylic acid)

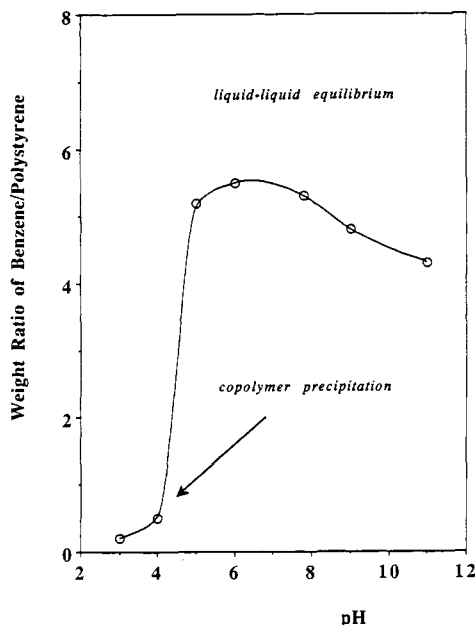


Figure 2. Solubilization limits of benzene into micelles expressed as the weight ratio of benzene to polystyrene (ξ_B) as a function of pH 3–11. ($c = 3 \times 10^{-3} \text{ g cm}^{-3}$; $I = 0.1$).

micelles were obtained by determining the saturation limits in a series of buffer solutions in the range pH 3–11. In Figure 2, the solubilization limits for a constant copolymer concentration ($c = 3 \times 10^{-3} \text{ g cm}^{-3}$) and a constant ionic strength ($I = 0.1$ with KCl) are given as a function of pH. These data show a representative and general trend of decreasing stability and solubilization capacity with increasing acidity of the aqueous medium.

Changes in micellar size that resulted from the solubilization of increasing amounts of benzene were monitored by QELS measurements of R_H . Interpretation of changes in R_H is not as straightforward as in the systems studied by Tontisakis et al.^{5c} It appears that solubilization generally occurs simultaneously into micellar cores and into shells. The latter effect is suppressed at pH ≥ 9 ; nevertheless, experimental evidence suggests that, even at high pH, a certain amount of a nonpolar substance may be solubilized into the micellar shell.¹³ While micellar cores may swell upon benzene adsorption, shells may partially collapse with the induced formation of hydrophobic domains. The hypercoiling of highly concentrated and possibly strongly interpenetrated poly(methacrylic acid) chains may be expected to produce a considerable decrease in shell thickness. Moreover, the "structural changes" in the shells at neutral and lower pHs depend significantly on the conditions of solubilization (i.e., the increments of benzene added and the interval between additions).

Solubilization at pH 9–11 provides relatively direct information on the swelling of the micellar cores. In this case, the repulsion of ionized carboxylic groups inhibits the formation of hydrophobic domains in the shell, and it is reasonable to believe that benzene is solubilized mostly into the core. The degree of dissociation in the highly concentrated poly(methacrylic acid) blocks near the core/shell interface does not have to be the same as at the shell periphery⁸ⁱ such that small changes in the shell structure cannot be completely ruled out, and this may influence our assessment of the core behavior. In Figure 3, $2R_H$ is shown as a function of ξ_B in micellar cores for two different solubilization rates, or more precisely for two different benzene increments: (1) 1-h intervals between 1- μL

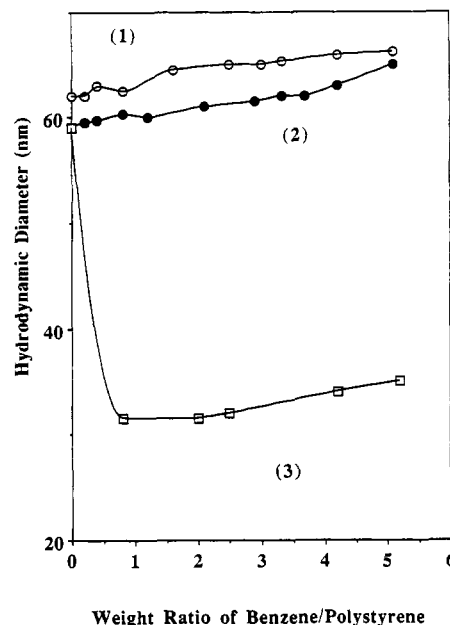


Figure 3. Hydrodynamic diameter ($2R_H$) of D1-SMA micelles in aqueous buffers as a function of the weight ratio of benzene to polystyrene (ξ_B): curve 1, independent of solubilization rate, $c = 5 \times 10^{-3} \text{ g cm}^{-3}$, pH 9, $I = 0.1$; curve 2, for slow solubilization rate, $c = 2 \times 10^{-3} \text{ g cm}^{-3}$, pH 7.9, $I = 0.1$; curve 3, for faster solubilization rate, $c = 2 \times 10^{-3} \text{ g cm}^{-3}$, pH 7.9, $I = 0.1$.

additions per 4 mL of micellar solution and (2) 1-h intervals between 3- μL additions. Also shown is one case that is independent of solubilization rate. Figure 3, curve 1, shows R_H of the micelles at pH 9 changes only slightly with increasing ξ_B in a region that spans 30–34 nm and does not depend on the solubilization rate. These small changes reflect mainly an increase in a core radius because solubilization into the shell is suppressed and the shell thickness should not change appreciably. The core diameter is initially smaller than ca. 10 nm; thus, a change of ca. 4 nm is quite significant. The data from samples in neutral buffers (pH 5–8) with the modest ionic strength ($I = 0.1$) show surprising behavior. In Figure 3, curve 2, we see that when benzene is added slowly (in 1- μL increments), the R_H are similar to those at high pH. If benzene is added faster (in 3- μL increments), a precipitous drop in R_H (ca. 50% of the original value) is observed immediately after the first benzene addition (Figure 3, curve 3). A small increase in micellar size is observed at higher ξ_B . The drop in R_H is a consequence of the induced hypercoiling of poly(methacrylic acid) chains. In this case, the local concentration of benzene exceeds that of the saturated benzene solution in water. The chemical potential of the bulk benzene (in microscopic droplets) differs from that in the saturated solution, and the solubilization mechanism from droplets into micellar shells may also differ from that which takes place in the aqueous phase. Measurements of R_H as a function of ξ_B carried out under various conditions (not shown here) show a strong dependence on pH, copolymer concentration, and solubilization rate.

Solubilization into Micellar Cores. A Study with Fluorescence Spectroscopy. In a companion paper,¹⁰ we demonstrated that the copolymer polystyrene-*block*-poly(methacrylic acid) (N4-SMA) forms a "sandwich" type excimer in good solvents due to the ability of the neighbor-pendant fluorescent groups to rotate freely in loose-chain coils. Chromophores may easily achieve the required "sandwich" arrangement during the monomer fluorescence lifetime. For the case of compact micellar cores, motions

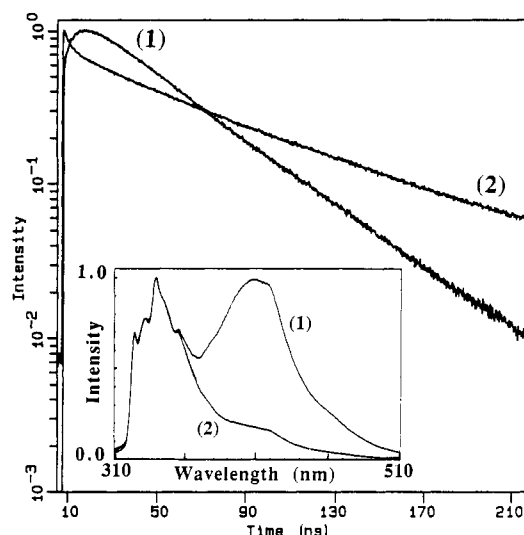


Figure 4. Normalized time-resolved excimer fluorescence decays for N4-SMA with excitation at 293 nm and emission at 410 nm: curve 1, in a good solvent 1,4-dioxane/CH₃OH (20 vol %); curve 2, N4-SMA micelles in water. Inset shows normalized steady-state spectra of N4-SMA with excitation at 293 nm and emission at 310–510 nm: curve 1, in a good solvent 1,4-dioxane/CH₃OH (20 vol %); curve 2, micelles in water.

of the chain as well as those of pendant groups are frozen and only a very low number of randomly oriented fluorophore groups are capable of excimer formation. Therefore, excimer fluorescence from micelles with naphthalene labels trapped in compact polystyrene cores is very weak. The time-resolved fluorescence decays for these micelles show no buildup and differ qualitatively from those in good solvents where a distinct buildup is observed. In Figure 4, the normalized steady-state fluorescence emission spectrum of N4-SMA in a good solvent (1,4-dioxane/methanol, 20 vol %; curve 1, inset) and in an aqueous solution of micelles (curve 2, inset) are shown and the normalized time-resolved excimer fluorescence for the same cases is compared. The classic buildup into the excimer state is clearly present for the copolymer in good solvent whereas for micelles only a weak and quenched fluorescence is observed from a small number of contact pairs that form excimers.

The monomer and excimer fluorescence decays for different quantities of solubilized benzene are shown in Figure 5, parts a and b, respectively. It is clear that until a specific (and quite large) quantity of benzene is solubilized, the swelling of micellar cores is not sufficient to liberate the rotational motions of pendant groups. It is reasonable that a relatively large amount of solubilized benzene is needed before we can see the onset of steady-state excimer fluorescence (Figure 6, curve 1) since two bulky adjacent pendant groups must simultaneously acquire a relatively high degree of rotational freedom. The excimer fluorescence buildup in micelles is slower ($\tau_{b-u} \approx 10$ ns) than that in a good solvent ($\tau_{b-u} \approx 7$ ns). Also shown in Figure 6 for comparison is the residual fluorescence anisotropy of mixed micelles of N1-SMA and SMA (see below). The residual anisotropy is a continuous function of added benzene and decreases steadily until $\xi_B \approx 3$, whereas I_E/I_M is approximately constant in the same range.

Data describing the mobility of polymer chains and pendant groups in micellar cores¹⁴ were also obtained from time-resolved anisotropy measurements on the sample N1-SMA (which is similar to N4-SMA, except that it contains on average only 0.8 naphthalene group per polymer chain).

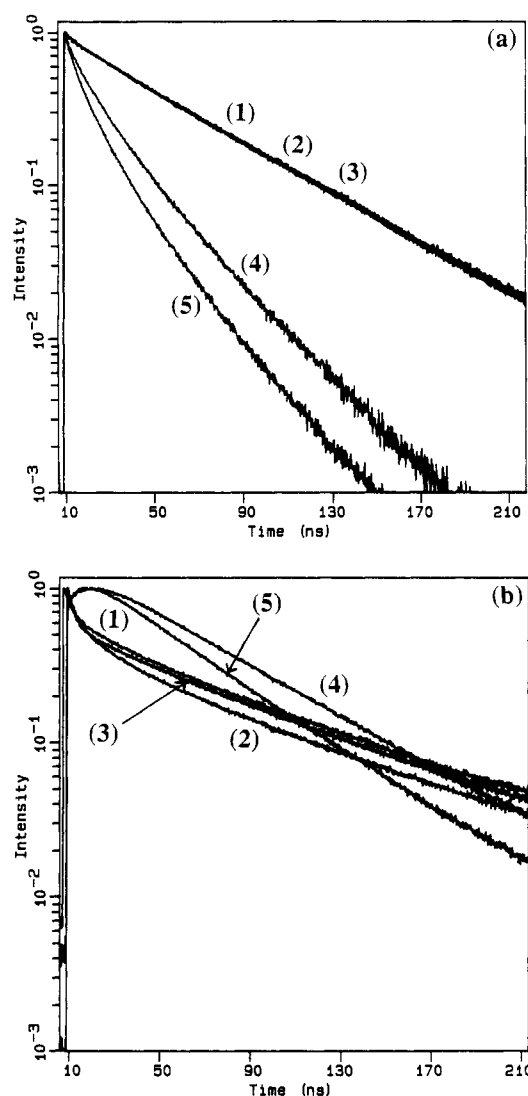


Figure 5. (a) Time-resolved monomer fluorescence decays from N4-SMA micelles in water ($c = 2 \times 10^{-3}$ g cm⁻³) for different weight ratios of solubilized benzene with excitation at 293 nm and emission at 340 nm: curve 1, $\xi_B = 0$; curve 2, $\xi_B = 0.9$; curve 3, $\xi_B = 2.4$; curve 4, $\xi_B = 4.4$; curve 5, $\xi_B = 5.9$. (b) Time-resolved excimer fluorescence decays from N4-SMA micelles in water for the same conditions as Figure 5a with excitation at 293 nm and emission at 410 nm.

The anisotropy decay for N1-SMA in a good nonviscous solvent (1,4-dioxane/methanol, 20 vol %) is quite fast, and almost no residual anisotropy is detected (spectrum not shown). This is expected given that the probe is located at the end of the polystyrene block. The data were fit using a multiexponential function described by

$$r(t) = r_0 \sum A_i \exp[-t/\tau_{ri}] + r_\infty \quad (5)$$

where τ_{ri} are the effective rotation correlation times ($\tau_{r1} = 90$ ps, $\tau_{r2} = 934$ ps) of the distinguishable depolarization modes, A_i are the preexponential factors ($A_{r1} = 0.774$, $A_{r2} = 0.213$), and r_0 and r_∞ are the initial and the residual anisotropies, respectively ($r_\infty \approx 0$). While our value of $r_0 = 0.35$ is lower than the theoretical value of 0.4 for parallel absorption and emission transition dipole moments, the difference is relatively small and does not inhibit our ability to draw reasonable conclusions concerning the data described herein. This discrepancy is likely a consequence of the complicated photophysics of naphthalene derivatives (see following) together with the limitations of the experimental setup. Laser instability during measurements (typically 2–3 h for one anisotropy curve) and the

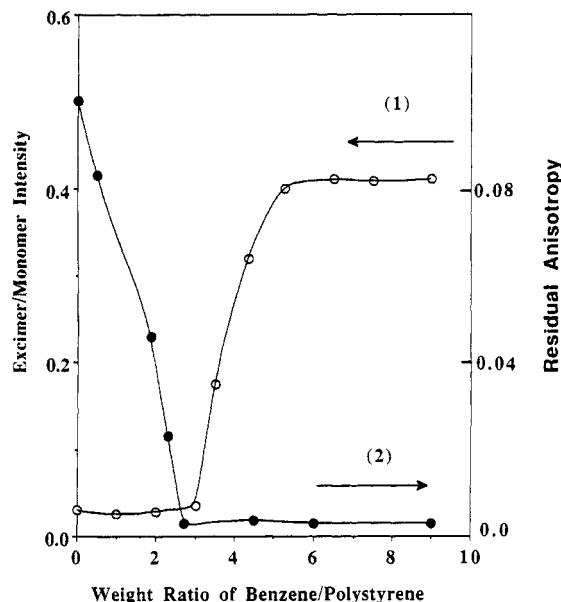


Figure 6. Steady-state excimer to monomer emission (I_{410}/I_{340}) (curve 1), $c = 2 \times 10^{-3} \text{ g cm}^{-3}$, for N1-SMA micelles and residual anisotropy (r_∞) (curve 2), $c = 6 \times 10^{-3} \text{ g cm}^{-3}$, for mixed micelles of N1-SMA and SMA. Both curves are functions of the weight ratio of benzene to polystyrene (ξ_B).

wavelength dependence of the microchannel plate^{15a} result in a small uncertainty in the determination of time $t = 0$. For very fast anisotropy decays, even small shifts in the beginning of the decay, corresponding to the width of one channel (ca 6.7 ps), may cause considerable errors in r_0 ($\Delta r_0 > 0.05$). Also, the current configuration of our system precludes any excitation close to 320 nm where the weak S_0 - S_1 absorption of naphthalene is located. Our excitation at 293 nm produces the S_2 excited state, and a slight partial internal depolarization of the emission takes place during the rapid vibrational relaxation to vibrational states S_1 which have a different symmetry from S_2 .

For this work, the value $r_0 = 0.35$ was confirmed by measuring both the labeled and nonhydrolyzed sample in a mixture of mineral oil and dibutyl terephthalate and of 2-methylnaphthalene in mineral oil where the slow anisotropy decay allows one to determine the value of r_0 unambiguously.

The interpretation of anisotropy decay curves for naphthalene labels in micelles composed solely of N1-SMA must be performed cautiously because of the likelihood of donor to donor energy migration which results in additional depolarization. In micellar cores, it is likely that there exists a nonhomogeneous free-end distribution including clusters of naphthalenes. In an aqueous solution of N1-SMA micelles, we observe a fast partial depolarization (≤ 100 ps) with a constant but relatively low residual anisotropy (ca. 0.05, curves not shown). This suggests a nonhomogeneous spatial distribution of fluorophores. After saturation by benzene, the anisotropy rapidly decays essentially to zero residual anisotropy, indicating relatively free rotation. It is also possible that after the pendant group motion is liberated, the proper orientation for efficient energy migration may be easily reached, which also increases the depolarization rate.

To suppress the effect of donor to donor energy migration and subsequent depolarization, two types of mixed micelles were prepared and studied: (1) M1 containing 20 wt % labeled copolymer N1-SMA and 80 wt % nonlabeled copolymer SMA and (2) M2 containing 10 wt % labeled copolymer N1-SMA and 90 wt % nonlabeled copolymer SMA. The molar mass of the nonla-

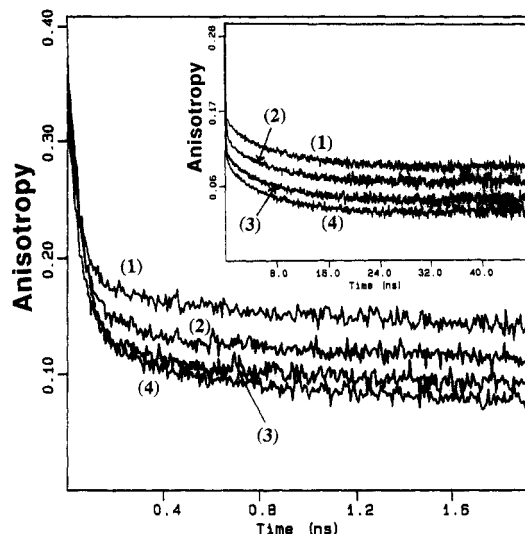


Figure 7. Time-resolved anisotropy decays (short time scale) of aqueous solutions of mixed micelles M1 (20 wt % labeled sample N1-SMA with 80 wt % nonlabeled sample SMA, overall copolymer concentration $3 \times 10^{-3} \text{ g cm}^{-3}$) for different weight ratios of benzene to polystyrene (ξ_B) with excitation at 293 nm and emission at 340 nm: curve 1, $\xi_B = 0$; curve 2, $\xi_B = 0.5$; curve 3, $\xi_B = 1.2$; curve 4, $\xi_B = 1.8$. Inset: same curves on a long time scale.

beled copolymer SMA is slightly lower ($M_w = 5.78 \times 10^4 \text{ g mol}^{-1}$) than that of the labeled sample N1-SMA, but the relative content of the blocks is virtually the same (the molar fraction of polystyrene units $x_S = 0.60$). Mixed micelles were prepared by mixing the amorphous samples in the required ratios and by dissolving in a 1,4-dioxane (80 vol %)/ H_2O mixture. The micellization equilibrium is not frozen in this case, and a unimers/micelles mass exchange occurs. Mixed micelles may also be formed by mixing two different micellar solutions in 1,4-dioxane-rich solvents as was shown from ultracentrifugation measurements.¹⁶ In our study, the labeled and nonlabeled micelles are quite similar and therefore indistinguishable by ultracentrifugation; the tendency to form mixed micelles in this case is extremely high since labeling by naphthalene changes the copolymers very little. Therefore, it is reasonable to assume that the labeled and nonlabeled copolymers are distributed uniformly in the ensemble of micelles studied here. In Figure 7, the time-resolved anisotropy decays for micelles M1 (total copolymer concentration $c = 3 \times 10^{-3} \text{ g cm}^{-3}$) with increasing amounts of solubilized benzene are shown. All fluorescence measurements for mixed micelles M1 and M2 were very similar to each other.

In micelles without benzene added, the residual anisotropy is higher than that of micelles formed exclusively from the N1-SMA, but still is quite low ($r_\infty \approx 0.1$). At least three exponentials are required to fit the anisotropy decays for naphthalene emission. All occur on a short time scale, and their contribution is too large for motion in a glassy state. The lifetimes and preexponential factors of the two more rapid processes ($\tau_{11} = 55 \text{ ps}$, $A_1 = 0.48$; $\tau_{12} = 2.2 \text{ ns}$, $A_2 = 0.11$) are quite similar to those observed in a good solvent, and the slower one ($\tau_{13} = 49 \text{ ns}$, $A_3 = 0.41$) is comparable, for example, with segmental motions in polyisoprene rubber at moderately elevated temperatures.¹⁷ Investigation of this problem is still under way, and interpretation of the curves will be given later (essentially the same decay was observed for a film cast from these same micelles in a selective solvent mixture of 1,4-dioxane/methanol).¹⁸ However, the effect of the core swelling is quite evident in the residual anisotropy

presented in Figure 7, and it is in agreement with the excimer formation study. As the fluorophore motions are liberated with an increasing amount of solubilized benzene, the residual anisotropy decreases. The decrease is gradual and is easily observed at a lower ξ_B than required for changes in the excimer/monomer fluorescence ratio (see Figure 6, curve 1).

Solubilization into Hydrophobic Domains in Poly(methacrylic acid) Blocks. Preliminary Measurements with Fluorescence Spectroscopy. In the above, we concentrated on the effect of the solubilized nonpolar compound on the micellar cores. The results of all experimental techniques applied to the study of the micellar shells to date also indicate very complex behavior upon absorption of benzene. We believe that measurements for one type of label cannot result in a complete explanation of the observed behavior of the poly(methacrylic acid) shells. Various fluorophores (sorbed as well as covalently attached to the copolymer) which are sensitive to microenvironment polarity (mainly to local pH) must be used to fully understand the shell behavior and structure. To be able to evaluate perturbations on the system caused by the presence of a fluorophore, a series of fluorophores with different polarities should be studied.

We are continuing to investigate the shell behavior, and the results will be presented later.¹⁸ Here we present some preliminary findings from dansyl-labeled copolymer micelles which are relevant to this solubilization study. The data presented are quite complex and serve to illustrate some of the problems encountered when working with the dansyl system D1-SMA.

Structural changes in poly(methacrylic acid) shells during the solubilization of benzene were studied by fluorimetry using the copolymer D1-SMA. Dansyl groups are attached to the ends of poly(methacrylic acid) blocks, and due to hydrolysis by HCl, a considerable fraction of the amino groups are protonated. As a result of their relatively nonpolar nature and a random distribution of the free-block ends, it appears that some dansyls are exposed to the aqueous microenvironment whereas others are hidden in hypercoiled-hydrophobic structures in the shells. Both the quantum yield and emission wavelength of this probe depend strongly on the microenvironment polarity.

The steady-state spectra of D1-SMA micelles in water are quite complicated, depend strongly on the excitation wavelength, and are difficult to interpret (see Figure 8a). For this system, the protonated and deprotonated forms must be considered for both excitation and emission spectra. Excitation of protonated dansyl results in subsequent dissociation as the acidity of the protonated amino group increases strongly upon excitation.^{9b} The emission spectrum for excitation of protonated dansyl at 275 nm shows several narrow peaks in the region 375–430 nm and a broad peak with a maximum at 490 nm from dansyl which is strongly polarity dependent (emission in water is at 580 nm).^{9b} Also, a blue shift was observed, indicating that a considerable fraction of dansyl labels experience a much less polar microenvironment than in water. The strong polarity dependence along with the presence of protonated and deprotonated forms makes it difficult to arrive at any unambiguous conclusions concerning the location of the dansyl groups.

Time-resolved anisotropy measurements (excitation at 293 nm, emission at 375 nm) were also employed to study this system (see Figure 8b). The decays for the micelles in water have a complex shape and cannot be described by a simple rotation of probes in an homogeneous medium.

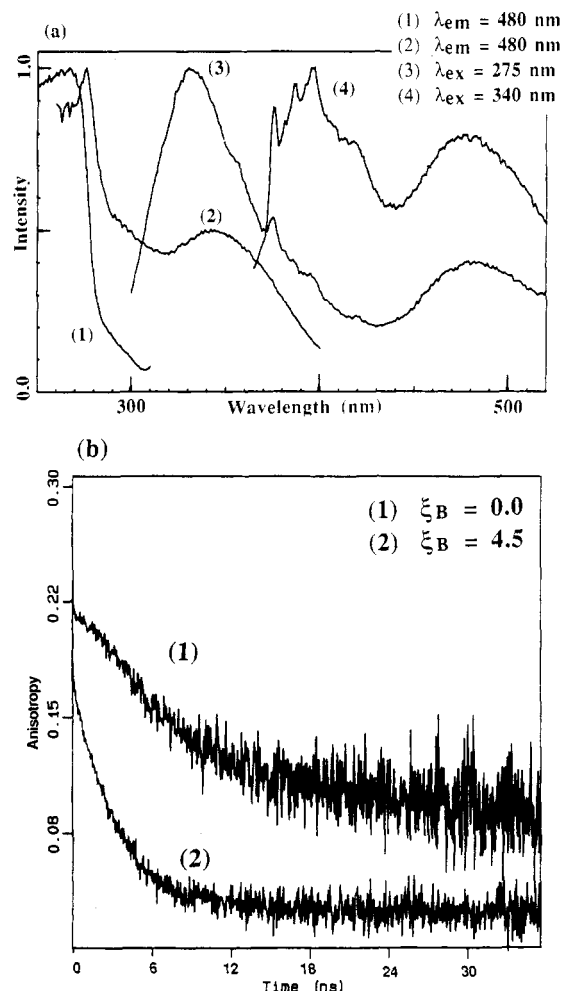


Figure 8. (a) Steady-state spectra of D1-SMA micelles in water: excitation spectra of protonated form with emission at 480 nm (curve 1) and deprotonated form with emission at 480 nm (curve 2); emission spectra of protonated form with excitation at 275 nm (curve 3) and deprotonated form with excitation at 340 nm (curve 4). (b) Time-resolved anisotropies for D1-SMA micelles in water with excitation at 293 nm and emission at 375 nm: curve 1, $\xi_B = 0$; curve 2, $\xi_B = 4.5$.

It seems likely that a model that assumes one type of probe for which the fluorescence lifetimes and rotational correlation times are different¹⁹ may be used to describe such decays. We believe that it is likely that a certain fraction of free-block ends are coiled back into the shell and those dansyl groups would probably experience a lower polarity of the microenvironment and have their mobility be restricted. On the other hand, some dansyls may be stretched out from the shell where they are exposed to water such that both their lifetime and rotation correlation time are shorter. The solubilization of benzene apparently liberates the motions of dansyl and its interactions with the various microenvironments because the anisotropic decay changes from a very complex decay to a typical simple decay (see Figure 8b). Again, these data are difficult to interpret accurately at this time because of the complications due to the dansyl probe. Later work will emphasize other probes bound to the micelle shell. The aforementioned brief descriptions of the steady-state and time-resolved fluorescence data are not for the purpose of drawing exact conclusions at this time but serve to illustrate the difficulties encountered in the investigation of the complex behavior of micellar shells using the D1-SMA system.

Study of the Polyelectrolyte Shell. A Study with QELS. QELS was used to investigate a number of features

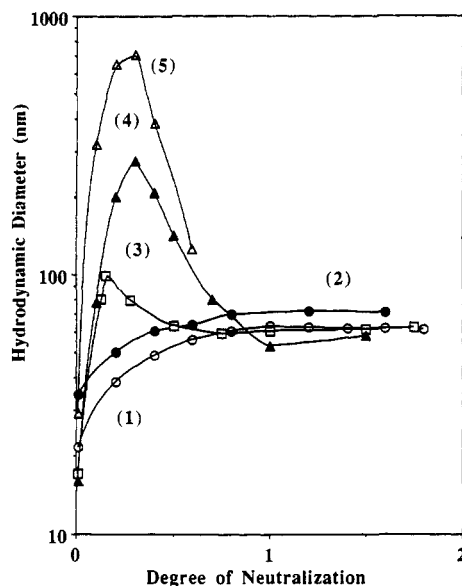


Figure 9. Apparent hydrodynamic diameter ($2R_H$) for different concentrations of aqueous solutions of micelles D1-SMA as functions of the degree of neutralization: curve 1, $c = 1.5 \times 10^{-3} \text{ g cm}^{-3}$; curve 2, $c = 3 \times 10^{-3} \text{ g cm}^{-3}$; curve 3, $c = 5 \times 10^{-3} \text{ g cm}^{-3}$; curve 4, $c = 6.6 \times 10^{-3} \text{ g cm}^{-3}$; curve 5, $c = 1 \times 10^{-2} \text{ g cm}^{-3}$.

of these copolymer systems. These features include the complex solubilization processes in the shell, the effects caused by the electrolyte nature and by "specific interactions" in the water-soluble poly(methacrylic acid) block, and the behavior of micelles at various degrees of neutralization for low ionic strength ($I = 0.01$) and in a broad region of pHs at high ionic strength ($I = 0.1$).

The apparent hydrodynamic diameter ($2R_H$) of micelles D1-SMA at different copolymer concentrations are shown in Figure 9 as a function of the degree of neutralization (α) for low ionic strength (no other salt added). For low copolymer concentrations, the $2R_H$ values monotonously rise with increasing α as parts of the poly(methacrylic acid) blocks in the shell stretch out due to the electrostatic repulsion of ionized COO^- groups (these are not compensated by an excess concentration of small cations). At higher copolymer concentrations, the shapes of R_H vs α curves change dramatically. The apparent values of R_H reach a very high and steep maximum at $\alpha = 0.25\text{--}0.35$ and show a high apparent polydispersity ($\mu_2(q)/[\Gamma(q)]^2$) of ca. 0.1–1.5. The autocorrelation curves ($g^{(1)}(t, q)$) are very nonexponential, and the decay at early times is significantly faster than at later times.

The relative viscosities of the solutions with copolymer concentration $c = 5 \times 10^{-3} \text{ g cm}^{-3}$ (and larger) show a very high maximum (Figure 10, curve 1), and the relative integrated intensity of the scattered light (I/I_0 , where I_0 is the intensity before titration) shows a minimum (Figure 10, curve 2). These observations suggest that the repulsion of highly charged spherical micelles with stretched polyelectrolyte shells leads to the formation of partially organized structures in the solution. A similar phenomenon was reported for charged latex particles at much higher concentrations.^{7d}

Analysis of the Laplace transform of the autocorrelation curve ($g^{(1)}(t, q)$) gives a broad spectrum of correlation times with two well-separated maxima. Measurements in the broad angular range $30\text{--}150^\circ$ indicate that both modes are diffusion-controlled processes. The corresponding diffusion coefficients differ by a factor of ca. 30 ($D_1 = 6.96 \times 10^{-7} \text{ cm}^2 \text{ s}^{-1}$, $D_2 = 2.30 \times 10^{-8} \text{ cm}^2 \text{ s}^{-1}$). The corresponding values for low micellar concentration ($c = 1.5$

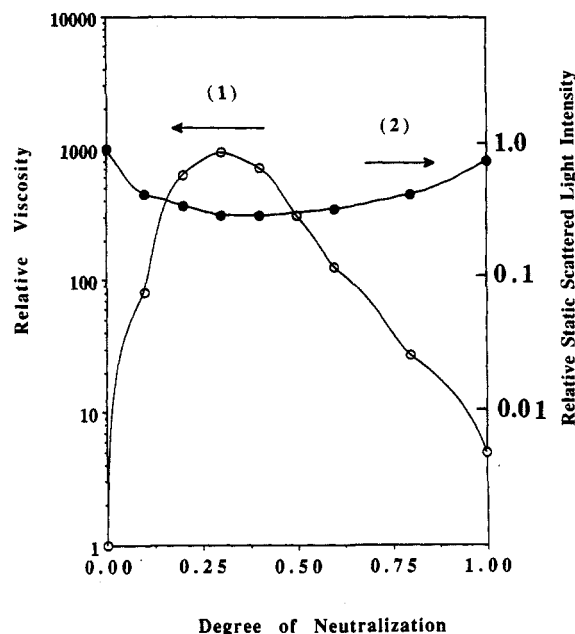


Figure 10. Relative viscosity (η/η_0) (curve 1), where η_0 is the viscosity before titration, and relative static scattered light intensity (I_{90}/I_{90}^0) (curve 2), where I_{90}^0 is the intensity for the solution before titration. Both are for an aqueous solution of D1-SMA micelles with $c = 6.6 \times 10^{-3} \text{ g cm}^{-3}$, and both are functions of the degree of neutralization.

$\times 10^{-3} \text{ g cm}^{-3}$) where long-range interactions are nearly negligible are $D = 1.12 \times 10^{-7} \text{ cm}^2 \text{ s}^{-1}$ in pure water and $D = 1.11 \times 10^{-7} \text{ cm}^2 \text{ s}^{-1}$ in a buffer solution (pH 4, $I = 0.1$). It is likely that the fast-diffusion mode describes the so-called "collective diffusion" which was observed in semidilute polyelectrolyte solutions and latex particles^{7d} where a certain degree of long-range order is assumed. The slow motion may correspond to the individual diffusion of clusters of structurally organized micelles. The experimental setup used does not permit us to draw a more detailed conclusion. Nevertheless, destructive structural interference diminishing the scattered intensity supports the concept of a partial long-order structural organization of highly charged and expanded spherical particles. At the same time, there are two distinct diffusion modes along with extrema in various quantities which differ by orders of magnitude from the values obtained for higher ionic strength. This interesting phenomenon is the subject of a new study.

Summary

The results of numerous experimental techniques show that the behavior of polystyrene-*block*-poly(methacrylic acid) is quite unique when compared to that of nonpolar micelles in organic solvents and that of water-soluble polymer micelles which do not contain polyelectrolyte shells. The properties and stability of micellar systems are strongly influenced by the hydrophobic-hypercoiling of poly(methacrylic acid) blocks in the shells in buffers with a low pH or at low degrees of ionization in pure water. Decoiling and expansion of segments of charged chains which contain the dissociated carboxylic groups improve the free energy balance of the system and increase micellar stability. Solubilization experiments at elevated pHs suggest that the local dissociation of carboxylic groups in highly concentrated poly(methacrylic acid) in shells is changing from the shell periphery toward the core/shell interface and does not correspond to the pH of the buffer.

Acknowledgment. This work was sponsored by the Department of the Army (Grant No. DAAA L03-90-G0147). S.E.W. acknowledges the financial support of the National Science Foundation Polymer Program (Grant No. DMR 9000562).

References and Notes

- (1) (a) Chandar, P.; Somasundaran, P.; Turro, N. J. *Macromolecules* **1988**, *21*, 950. (b) Chu, D.-Y.; Thomas, J. K. *J. Am. Chem. Soc.* **1986**, *106*, 6270. (c) Turro, N. Y.; Baretz, B. H.; Kuo, P.-L. *Macromolecules* **1984**, *17*, 1321. (d) Wilhelm, M.; Zhao, Ch.-L.; Wang, Y.; Xu, R.; Winnik, M. A.; Mura, J.-L.; Riess, G.; Croucher, M. D. *Macromolecules* **1991**, *24*, 1033. (e) Prochazka, K.; Bednar, B.; Svoboda, P.; Trnena, J.; Mukhtar, E.; Almgren, M. *J. Phys. Chem.*, in press. (f) Major, M. D.; Torkelson, J. M.; Brearley, A. M. *Macromolecules* **1990**, *23*, 1700.
- (2) (a) Hsu, L.-J.; Strauss, U. P. *J. Phys. Chem.* **1987**, *91*, 6238. (b) Chu, D.-Y.; Thomas, J. K. *Macromolecules* **1987**, *21*, 1387.
- (3) Binana-Limbele, W.; Zana, R. *Macromolecules* **1987**, *20*, 1331; **1990**, *23*, 273.
- (4) (a) Tuzar, Z.; Bahadur, P.; Kratochvil, P. *Makromol. Chem.* **1981**, *182*, 1751. (b) Molau, G. E.; Wittrod, W. M. *Macromolecules* **1968**, *1*, 260. (c) Price, C.; Stubbersfield, R. B. *Eur. Polym. J.* **1987**, *23*, 1987.
- (5) (a) Nagarajan, R.; Barry, M.; Ruckenstein, E. *Langmuir* **1986**, *2*, 210. (b) Nagarajan, R.; Ganesh, C. *Macromolecules* **1989**, *22*, 4312. (c) Tontisakis, A.; Hilfiker, R.; Chu, B. *J. Colloid Interface Sci.* **1990**, *135*, 427. (d) Al-Saden, A. A.; Whateley, T. L.; Florence, A. T. *J. Colloid Interface Sci.* **1982**, *90*, 1033.
- (6) Cogan, K. A.; Gast, A. P. *Macromolecules* **1990**, *23*, 745.
- (7) (a) Pleštil, J.; Ostanevich, Yu. M.; Bezzabotonov, V. Yu.; Hlavata, D.; Labsky, J. *Polymer* **1986**, *27*, 839. (b) Sedlak, M.; Konak, C.; Stepanek, P.; Jakes, J. *Polymer* **1987**, *28*, 873. (c) Sedlak, M.; Konak, C.; Stepanek, P.; Jakes, J. *Polymer* **1990**, *31*, 253. (d) Stepanek, P.; Konak, C. *Adv. Colloid Interface Sci.* **1984**, *21*, 195, and the references in parts IV.A. and IV.D.
- (8) (a) Katchalski, A.; Eisenberg, M. *J. Polym. Sci.* **1950**, *6*, 145. (b) Katchalski, A. *J. Polym. Sci.* **1951**, *7*, 39. (c) Bednar, B.; Morawetz, H.; Shafer, J. A. *Macromolecules* **1984**, *17*, 1634. (d) Bednar, B.; Morawetz, H.; Shafer, J. A. *Macromolecules* **1985**, *18*, 1940. (e) Bednar, B.; Li, Z.; Huang, Y.; Chang, L.-C. P.; Morawetz, H. *Macromolecules* **1985**, *18*, 1829. (f) Fidler, V.; Vajda, S.; Limpouchova, Z.; Dvorak, J.; Prochazka, K.; Bednar, B. *Collect. Czech. Chem. Commun.* **1989**, *54*, 3011. (g) Bednar, B.; Trnena, J.; Svoboda, P.; Vajda, S.; Fidler, V.; Prochazka, K. *Macromolecules* **1991**, *24*, 2054. (h) Chu, D.-Y.; Thomas, J. K. *Macromolecules* **1987**, *20*, 2133; *J. Phys. Chem.* **1985**, *89*, 4065. (i) For further details, see refs 1–28 in: Chu, D.-Y.; Thomas, J. K. *ACS Symp. Ser.* **1987**, *358*, 434. (j) Liu, G.; Guillet, J. E.; Al-Takrity, E. T. B.; Jenkins, A. D.; Walton, D. R. M. *Macromolecules* **1991**, *24*, 68.
- (9) (a) Dubin, P. L.; Strauss, U. P. *J. Phys. Chem.* **1970**, *74*, 2842. (b) Strauss, U. P.; Vesnauer, G. *J. Phys. Chem.* **1975**, *79*, 1558, 2426. (c) Strauss, U. P.; Schlesinger, M. S. *J. Phys. Chem.* **1978**, *82*, 1627.
- (10) Prochazka, K.; Kiserow, D.; Ramireddy, C.; Tuzar, Z.; Munk, P.; Webber, S. E. Preceding paper in this issue.
- (11) This is the actual time during which the TAC and MCB process data.
- (12) Prochazka, K.; Glockner, G.; Hoff, M.; Tuzar, Z. *Makromol. Chem.* **1979**, *185*, 1187.
- (13) The transient absorption spectra of pyrene solubilized into micelles show pyrene cation absorption at low and high pH under high laser energy excitation at 308 nm. Photoionization and cation formation require a polar environment and have been observed in aqueous solutions of poly(methacrylic acid) at low and neutral pHs but have never been observed in nonpolar media such as heptane or toluene or in polystyrene films. The pyrene solubility in water is so low that possible cation absorption is below the detection limit of the experimental technique and was not detected. Hsiao, J. Unpublished data.
- (14) In the relatively dense cores, the motion of the pendant group is strongly influenced by the motion of the chain segments and cannot be treated separately.
- (15) Lakowicz, J. R. *Principles of Fluorescence Spectroscopy*; Plenum Press: New York, 1986: (a) p 87; (b) pp 247–253.
- (16) (a) Munk, P.; Ramireddy, C.; Webber, S. E.; Tuzar, Z.; Prochazka, K.; Submitted to *Makromol. Chem.* (b) Tuzar, Z.; Webber, S. E.; Ramireddy, C.; Munk, P. *Polym. Prepr.* **1991**, *32* (1), 525.
- (17) Hyde, P. D.; Ediger, M. D.; Kitano, T.; Ito, K. *Macromolecules* **1989**, *22*, 2253.
- (18) Manuscript in preparation.
- (19) (a) Ludescher, R. D.; Peting, L.; Hudson, S.; Hudson, B. *Biophys. Chem.* **1987**, *28*, 59. (b) Birch, D. J. S.; Holmes, S.; Imhof, R. E. Time-Resolved Fluorescence Spectroscopy in Liquid Bilayers, presented at the 6th ICEET Conference, Prague, Czechoslovakia, 1989.

Registry No. C₆H₆, 71-43-2.